

# Experimental study of a $\Lambda$ -structure development and its transformation into the turbulent spot

G. R. Grek, V. V. Kozlov, M. M. Katasonov and V. G. Chernorai

Institute of Theoretical and Applied Mechanics SB RAS, Novosibirsk, Russia

**This paper presents the results of experimental research on the characteristics of  $\Lambda$ -structures, their development, and the mechanism of their transformation into turbulent spots. It has been shown that an isolated  $\Lambda$ -structure can damp as well as increase downstream and transform into a turbulent spot. The structure of the associated disturbances consists of two counter-rotating vortices (the 'legs' of disturbance) closed by a 'head' at the leading edge. The difference between the two types is that the  $\Lambda$ -structure that damps is a kind of a hairpin vortex which does not cross the upper boundary layer edge; the 'head' of the increasing  $\Lambda$ -structure crosses the upper boundary layer edge and the disturbance attains the form of the Greek letter  $\Lambda$ . It has been proposed that the increasing  $\Lambda$ -structure is connected with the development of secondary high frequency disturbances on the 'legs' of the structure. The reason for this is probably the local transverse velocity gradient  $\partial u/\partial z$  on the 'legs' of the  $\Lambda$ -structure, which creates conditions for the development of secondary disturbances in it. It has also been shown that the frequency of the secondary disturbance decreases because of the continuous extension of a localized disturbance under its downstream propagation. Secondary high frequency breakdown of structures is also observed when there is periodical generation.**

## Introduction

As is well known, the laminar-turbulent transition in the boundary layer at low free stream turbulence levels takes place with the appearance and development of the so-called Tollmien-Schlichting (TS) instability waves. At the nonlinear stage when the two-dimensional TS wave reaches high amplitudes, it transforms into typical three-dimensional structures resembling the Greek letter  $\Lambda$  in flow visualizations<sup>1</sup>. When these structures develop downstream, they cause turbulization of the flow. The mechanism of development and breakdown of  $\Lambda$ -structures is not clear yet. In classical transition whose linear stage is described by the linear theory of stability there are known to be two scenarios of  $\Lambda$ -structures appearing at the nonlinear stage: harmonic or Klebanoff

transition,  $K$ -mode<sup>2,3</sup> when in flow visualizations the structures are placed one after another<sup>1</sup>, and subharmonic or  $N$ -mode<sup>4,5</sup> when the structures are set as on a chess-board<sup>1</sup>. On the other hand  $\Lambda$ -structures are also observed in flow visualizations modelling other types of transition<sup>6</sup> and under natural conditions<sup>7</sup>.

Thus, the role of the longitudinal vortex structures ( $\Lambda$ -structures) in the transition process is important, and it is necessary to study them. Numerous theoretical and experimental research works explaining the nonlinear stage of classical transition make it possible to understand this mechanism. In particular it was found that the  $N$ -mode of transition occurs by nonlinear resonance interaction of the basic and two oblique waves with subharmonic frequency<sup>4,5</sup>. The  $K$ -mode of transition is more difficult to explain. Typical high frequency bursts (the so-called 'spikes' on the oscilloscope traces) were explained by the development of secondary high frequency disturbances on the local distortions of the profile of mean velocity caused by nonlinear development of a disturbance<sup>2</sup>. This fact was confirmed by a physical experiment<sup>8</sup>. However, the so-called resonance-wave concept<sup>9</sup> was suggested later on, in which the appearance of spikes was explained not by the secondary high frequency instability but by solitons generated near the upper boundary layer edge. Turbulization of the flow was performed by four-wave parametrical resonance which generated solitons. This concept was confirmed by numerical experiment<sup>10</sup>. It should be mentioned that this flow turbulization was experimentally confirmed only at the initial stages of nonlinear development of disturbances which can be described theoretically. The concept mentioned is still to be proved experimentally and theoretically for the later stages of transition of the flow into a turbulent state.

Modelling of classical transition was mainly connected with the generation of periodic disturbances in the boundary layer, i.e. introducing a harmonic wave. In the nonlinear transition stage a wave is transformed into three-dimensional  $\Lambda$ -structures which, propagating downstream, creates turbulence. It is known from research on 'natural' transition that in the majority of cases transition occurs through the stage of the formation and development of turbulent spots, i.e. structures localized in time and space. If localized  $\Lambda$ -structures

e-mail: grek@itam.nsc.ru

can be transformed into turbulent spots as in the above mentioned experiments, it is impossible to distinguish the given structures because of their close packing and their influence on each other. The study of turbulent spot formation is very important because it helps to understand transition in shear layers. Usually a turbulent spot is excited by powerful impulses in the boundary layer<sup>11</sup>, therefore the possibility of a turbulent spot appearing in the process of development of vortex disturbances was not studied. In ref. 12, an isolated  $\Lambda$ -structure was first modelled and it was shown that it was transformed into an isolated turbulent spot downstream. When the amplitude of the disturbance source decreased the disturbance was damped, but when the amplitude or flow velocity increased or with superimposition of high frequency periodic disturbances, the turbulent spot appeared again. In refs 13, 14 a hairpin vortex was investigated which was the same  $\Lambda$ -structure but more extended streamwise. It was shown that it consists of two counter-rotating vortices ('legs' of the structure) ending with a 'head' which crosses the upper boundary layer edge. As the structure propagates downstream secondary vortices are generated on its 'head' and 'legs', and it transforms into a turbulent spot.

The purpose of this work is to study in detail the transformation of an isolated  $\Lambda$ -structure into a turbulent spot and obtain qualitative and quantitative information on this mechanism.

### Experimental equipment and method of research

The research was performed in the low free stream turbulence wind tunnel T-324 of the Institute of Theoretical and Applied Mechanics, Siberian Branch of the Russian Academy of Sciences. The tunnel has a test section of transverse dimensions 1000 mm  $\times$  1000 mm and length of 4000 mm. A flat plate (1) made of acrylic plastic which is 1500 mm long, 1000 mm wide and 10 mm thick and vertically installed in the test section was used as the model. Disturbances were introduced in the boundary layer on the model through a slot (2) of 18 mm length and 0.4 mm width, set at a distance of 200 mm from the leading edge of the model (Figure 1). The slot was formed to create unequal distribution of intensity of the introduced disturbance along it (see ref. 12). Disturbances were introduced by a dynamic loudspeaker (3, 4). To generate high frequency disturbances a sinusoidal electrical signal with frequency of 200–250 Hz was transmitted to the loudspeaker (3) from the outlet of a special generator. Pulsed localized disturbance to generate an isolated  $\Lambda$ -structure was formed by the loudspeaker (4) to which short electric pulses of frequency 0.5–1 Hz were sent. To generate periodic  $\Lambda$ -structures the frequency of these pulses was raised to

60 Hz. Periodic and pulse signals were synchronized as one and the same generator was their source. In this experiment the flow velocity was 5.6 m/s, and the free stream turbulence was not more than 0.04%. Distribution of velocity in the boundary layer corresponded to Blasius flow.

All measurements were performed by a single hot-wire probe operating at constant temperature (5). The thickness of the probe wire was 6  $\mu$ m, the length was about 1 mm. The streamwise component of velocity fluctuations ( $u'$ ) and mean velocity ( $\bar{u}$ ) were measured at various points in  $x, y, z$  space (see Figure 1). The free stream velocity in the test section was measured by a Pitot-Prandtl probe connected to a bent liquid column micromanometer. The hot-wire probe was calibrated in a free flow against the Pitot-Prandtl tube at free stream velocities in the range 2–20 m/s in such a way that the error in the mean velocity was less than 3%. The calibration function is described by the formula

$$U = k_1(E^2 - E_0^2)^{1/n} + k_2(E - E_0)^{1/2}, \quad (1)$$

where  $E$  and  $E_0$  are output voltages of the anemometer at flow velocity  $U$  and zero, and  $k_1, k_2$  and  $1/n$  are constants determined empirically. The first term corresponds to the well-known King expression, and the second is added to allow for free convection at small flow velocities<sup>15</sup>.

Calibration of the hot-wire probe, collection, storing and processing of measured information were performed by a PC (Macintosh LC II) connected with the bridge of a DISA 55M01 hot-wire anemometer through an analog-to-digital converter (MacADIOS-ADIO, GW Instruments Company). The signal from the hot-wire anemometer probe comes to one inlet of the analog-to-digital converter. To the trigger input a signal from a low frequency source (short pulses with frequency of 0.5–1 Hz) was transmitted to preserve phase information of the disturbances investigated. Introduced into the

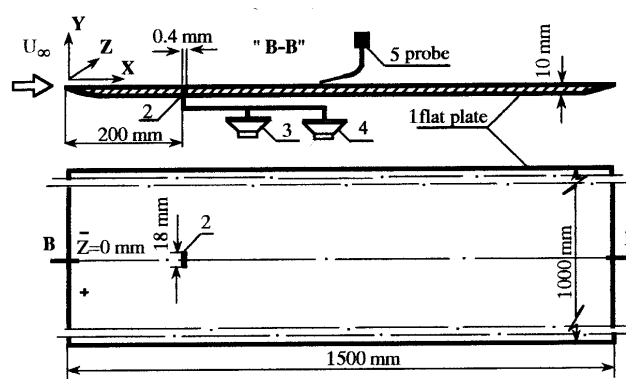


Figure 1. Experimental set-up.

computer, realizations of disturbance development in space and time were ensemble-averaged to improve the signal/noise ratio. This made it possible to distinguish a weak measured signal from undetermined noise. From 5 to 100 realizations were averaged depending on the level both of the selected signal and noise. Development of disturbances along the transverse coordinate  $z$  was measured in the region of maximum intensity in the direction  $y$  normal to the plate surface.

### Processing of measurement results

Measurement results were processed by a computer according to the program of space-time Fourier analysis. Space-time distribution of streamwise component of velocity was subject to Fourier-transformation in the space coordinate  $z$ :

$$u'(t, \beta) = (1/z_0) \int_{-z_0/2}^{z_0/2} e^{-i\beta z} u'(t, z) dz. \quad (2)$$

For various values of the coordinate  $x$  normalization was by the same quantity at  $z_0 = 128$  mm, which led to the same number of  $\mathbf{b}$ -harmonics for various sections along the longitudinal coordinate  $x$  (step-size in the transverse coordinate  $z$  was constant and equal to 1 mm). If the domain of measurement along  $z$  was less than +64 mm then on the left and (or) on the right zeroes were added in order to obtain the same quantity  $z_0$ . Since the function  $u'(z, t)$  is real, the amplitude part  $u'(t, \mathbf{b})$  is symmetrical in relation to  $\mathbf{b} = 0$ .

The results of calculations were presented in the form of contour diagrams of constant velocity fluctuations in the planes  $zt$ ,  $yt$  and  $yz$  for various values of the coordinate  $x$ . Solid isolines reflect velocity excess, dashed ones show defect. Deviations from the mean velocity shown by isolines are indicated by percentages in relation to the free stream velocity (min is a velocity defect, max is a velocity excess, step is interval between isolines); coordinate  $z$  is given in mm, time axis  $t$  is graduated in ms. Isolines are plotted with constant as well as variable steps by amplitude. In some cases experimental information is presented as distributions along the transverse and normal coordinates of the maximum amplitude of velocity pulses  $A = f(z)$ ,  $A = f(y)$ .

### Results of measurement

#### *Qualitative characteristics of development and transformation of $\Lambda$ -structure in a turbulent spot*

In the introduction it was said that the first results of the isolated  $\Lambda$ -structure transformation in a turbulent spot

were presented in ref. 12. The visualization picture of this process in the plane  $z$ - $x$  presented in this work demonstrates that the  $\Lambda$ -structure as well as the turbulent spot are well identified. As disturbance amplitude at the source was reduced, a turbulent spot did not appear and the disturbance was damped downstream. In Figure 2 taken from ref. 13, the oscilloscope traces are measured in the plane of symmetry of a localized disturbance depending on the streamwise coordinate  $x$  for two flow velocities. At  $U_\infty = 6.6$  m/s near the source of disturbances at  $x = 240$  mm ( $x_{\text{slot}} = 200$  mm), the oscilloscope trace shows a defect of velocity and the presence of high frequency natural disturbance with frequency  $f \approx 170$  Hz connected with  $\Lambda$ -structure formation. Oscilloscope traces further show that the disturbance decays downstream. On increase of flow velocity to  $U_\infty = 11$  m/s the disturbance changes radically downstream. First, the amplitude of the high frequency component of the disturbance increases sharply near the source ( $x = 240$  mm). Secondly, its development downstream transforms the previously damped localized disturbance into a turbulent spot. An increase of the amplitude of the disturbance introduced at the source without increasing flow velocity has the same result. The conclusion can be drawn that a high frequency 'natural seed' (connected probably with the tilting effect of an isolated wave in a shear flow) at the leading front of a localized disturbance may, under certain conditions, increase and lead to the transformation of a

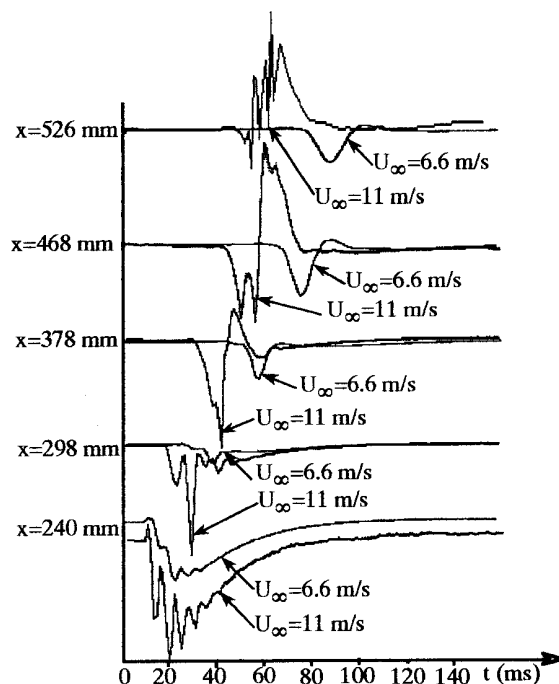


Figure 2. Oscilloscope traces of the  $\Lambda$ -structure development with a natural high-frequency disturbance at two free stream velocity,  $Z = 0$  mm.

damped localized disturbance into turbulent spot, as seen in the visualization picture<sup>12</sup>. As the localized disturbance propagates downstream, the frequency of the developing high-frequency secondary disturbance decreases ( $f \approx 130$  Hz and  $x = 468$  mm), probably due to streamwise stretching<sup>16</sup>. The conditions leading to an increase of a high-frequency natural disturbance in this structure, and the characteristics of its development, will be considered in detail in the next section, where an artificial disturbance will be studied and phase information makes it possible to obtain quantitative data.

At this stage we estimated only the main qualitative characteristics of  $\Lambda$ -structure transformation to a turbulent spot. After considering above the development of a natural high-frequency 'seed' in the localized disturbance, further results of research of a damped localized disturbance interacting with artificially introduced high-frequency disturbances will be presented. The results of similar research were published in ref. 17, where it was shown that in the interaction of two damped disturbances, namely a Tollmien-Schlichting (TS) wave and a  $\Lambda$ -structure, growing wave packet appears with frequency less than that of the T-S wave by a factor of 2, which is transformed to a turbulent spot downstream (Figure 3). Oscilloscope traces in Figure 4 (taken from ref. 13) demonstrate the development of a damped localized disturbance downstream as well as its interaction with a TS wave ( $f = 290$  Hz), ending in the formation of a turbulent spot. Qualitatively this process is similar to that of the development of a natural high-frequency 'seed' presented in the visualization picture of a  $\Lambda$ -structure transformation in a turbulent spot from ref. 12.

Thus, on the basis of the results of the research presented here we may state the following:

- (i) an isolated  $\Lambda$ -structure was modelled and various mechanisms of its transformation to a turbulent spot were qualitatively investigated; it was shown that the  $\Lambda$ -structure can damp downstream;

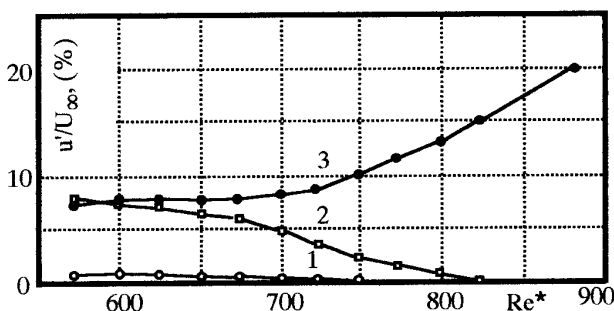


Figure 3. Curves for excitation growth (1 – Tollmien-Schlichting wave, 2 – localized disturbance, 3 – interaction of Tollmien-Schlichting wave with localized disturbance),  $y = y(u'_{\max})$ .

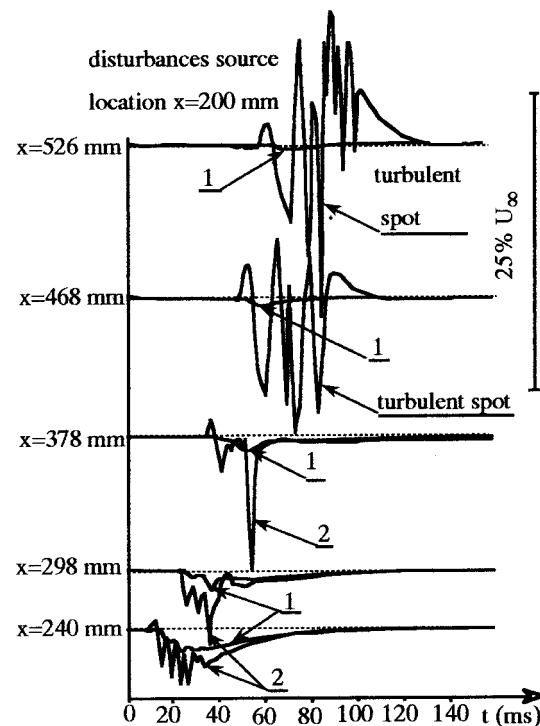


Figure 4. Oscilloscope traces of the downstream development of a decreasing  $\Lambda$ -structure (1) and a  $\Lambda$ -structure interacted with the high-frequency wave ( $f = 290$  Hz) (2),  $Z = 0$  mm.

- (ii) a damped  $\Lambda$ -structure can be transformed into a turbulent spot in case of a development of a 'seed' or in interaction with a high-frequency wave;
- (iii) since the  $\Lambda$ -structure stretches continuously in a shear layer, a high-frequency disturbance developing in it decays.

#### Quantitative characteristics of $L$ -structure development and transformation in a turbulent spot

The next stage of research of  $\Lambda$ -structure transformation in a turbulent spot was to study quantitative characteristics of the process in detail. Experiments were performed under the same conditions in which the visualization picture in ref. 12 was obtained. As already mentioned, in the absence of disturbances in the boundary layer, a laminar flow with mean velocity profile close to the Blasius was realized. The measured thickness of the boundary layer at distance  $x$  from the leading edge equal to 377, 480 and 587 mm was 5, 5.7 and 6.3 mm respectively. (It should be noted that the conditions of the given experiment and the visualization experiment presented in ref. 12 were the same.)

The distribution, along a spanwise coordinate, of the intensity of the localized disturbance introduced into the boundary layer,  $A_{\min}$ ,  $A_{\max}$ , is given in Figure 5a. The

diagram shows a peak in velocity defect in the plane of disturbance symmetry, and two peaks in excess velocity placed symmetrically in relation to the peak velocity defect. This distribution is typical of disturbances with two counter rotating vortices (Goertler vortices, hairpin and  $\Lambda$  vortices, etc.). The distributions show that disturbance damps downstream. The structure of the given damped localized disturbance is clearly illustrated by isolines of velocity fluctuations in the  $z$ - $t$  plane at  $y = y(u'_{\max})$  shown in Figure 5 *b-d*, in which the dashed lines show the region of velocity defect in the plane of symmetry, and solid lines show two regions of velocity excess on both sides of it. One can observe oblique waves on the edges of the disturbance, in the form of the isolines curved at a certain angle (dashed lines).

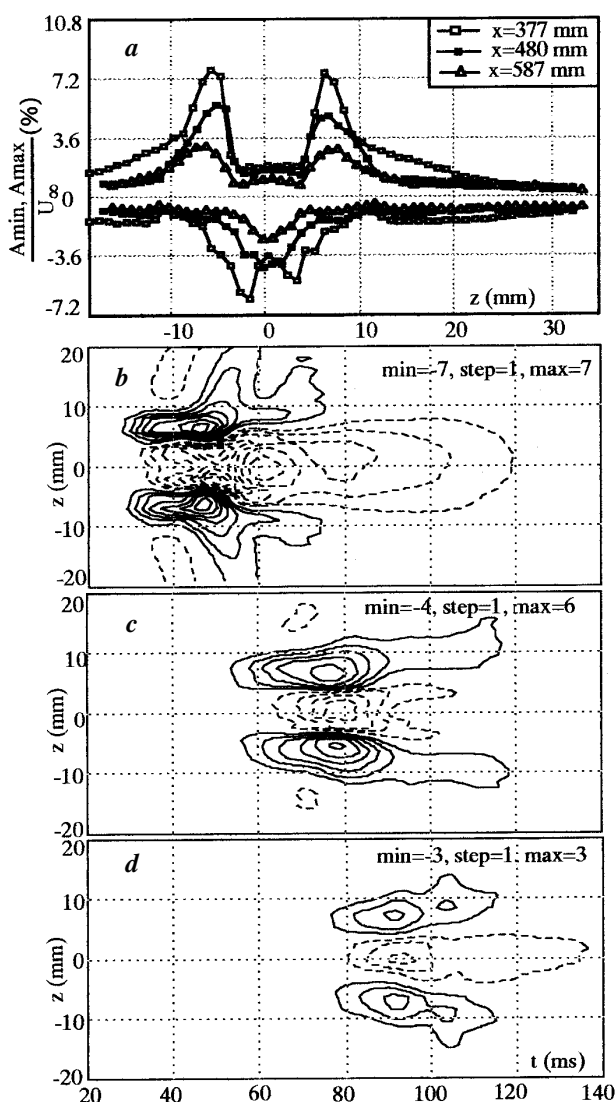


**Figure 5.** Spanwise distributions of the decreasing  $\Lambda$ -structure intensity depending on streamwise coordinate (*a*) and contour diagrams of constant velocity fluctuations of the  $\Lambda$ -structure in  $z$ - $t$  plane at  $x = 377$  mm (*b*), 480 mm (*c*), 587 mm (*d*);  $y = y(u'_{\max})$ ,  $U_{\infty} = 5.6$  m/s.

Propagating downstream, the disturbance damps. This is shown by a change of its maximum amplitude from 14% at  $x = 377$  mm (see Figure 5 *b*) to 6% at  $x = 587$  mm (see Figure 5 *d*).

A superimposed high-frequency periodic disturbance (with frequency  $f = 200$  Hz and amplitude  $A_{\text{RMS}}$  less than 1%) interacts with a localized disturbance leading to the growth of the latter, especially in the 'legs' region, i.e. in the counter-rotating vortices. It is shown by the intensity distribution of the localized disturbance and its interaction with a wave along the spanwise coordinate at  $x = 377$  mm (Figure 6 *a*) and in the isolines of velocity fluctuations of interacting disturbances in

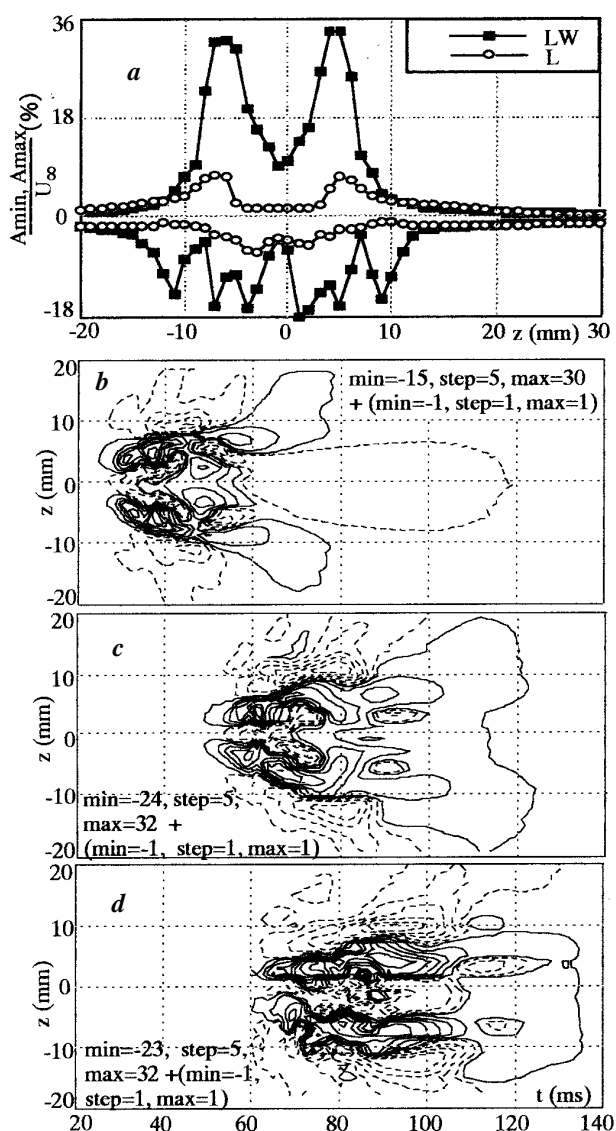


**Figure 6.** Spanwise distributions of the decreasing  $\Lambda$ -structure intensity (L) and its interaction with high-frequency wave (LW) depending on streamwise coordinate (*a*) and contour diagrams of constant velocity fluctuations of the  $\Lambda$ -structure interacted with the high-frequency wave ( $f = 200$  Hz) in  $z$ - $t$  plane at  $x = 377$  mm (*b*), 480 mm (*c*), 587 mm (*d*);  $y = y(u'_{\max})$ ,  $U_{\infty} = 5.6$  m/s.

the plane  $z-t$  at  $y = y(u'_{\max})$  shown in Figure 6 *b-d*. The amplitude of the localized disturbance on interaction with a wave increased by 4 times on the 'legs' of the structure (see Figure 6 *a*, at  $z = \pm 5$  mm) as compared to the amplitude of the disturbance without the wave. The structure of the 'legs' of the disturbance acquired a horseshoe shape with some periods of high frequency disturbance in them (see Figure 6 *b-d*). The amplitude of the disturbance (which is defined as the difference between max and min in each figure) rises downstream from 45% at  $x = 337$  mm to 56% at  $x = 480$  mm (see Figure 6 *b, c*) till the time when it is transformed to a turbulent spot at  $x = 587$  mm (Figure 6 *d*). The 'legs' of the localized disturbance stretch during its propagation downstream, which is why the frequency of the secondary high-frequency disturbance developing in them decreases continuously.

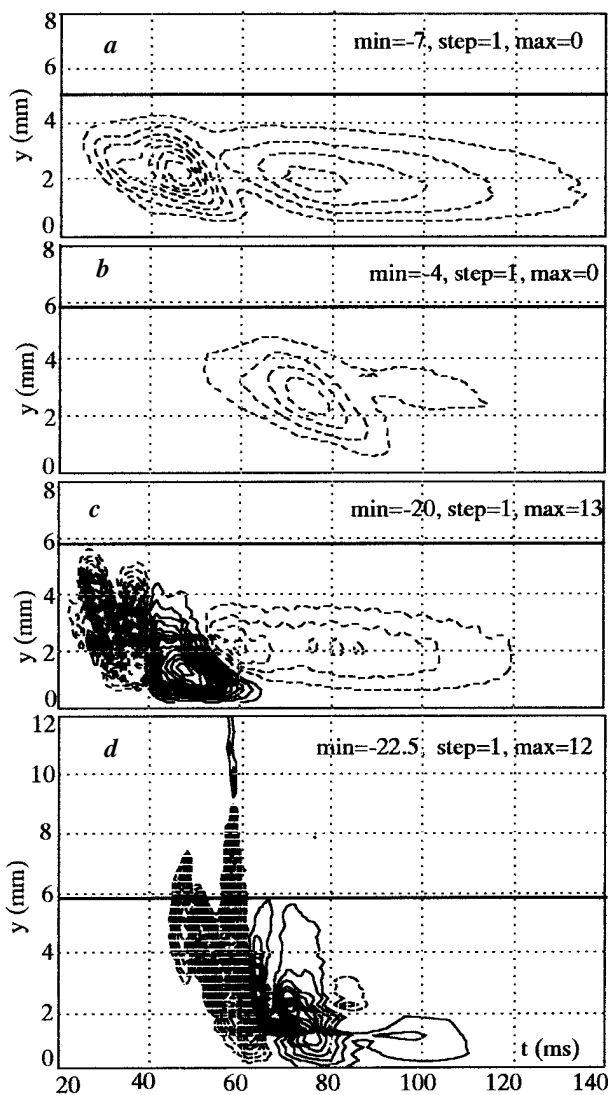


**Figure 7.** Contour diagrams of constant velocity fluctuations of the decreasing  $\Lambda$ -structure at  $x = 377$  mm (*a*),  $480$  mm (*b*) and its interaction with the high-frequency wave ( $f = 200$  Hz) at  $x = 377$  mm (*c*),  $480$  mm (*d*) in  $y-t$  plane at  $z = 0$  mm,  $U_{\infty} = 5.6$  m/s.

Comparing the intensity distributions of the localized disturbance and its interaction with the wave along the normal to the surface for various positions downstream (Figure 7), we may note the following features.

1. On the 'legs' of the 'decreasing' localized disturbance that interacts with the wave a region of excess velocity prevails, whose maximum intensity is near the wall (more detailed information is in ref. 18, especially figures 25, 30).
2. In the plane of symmetry, on the contrary, a velocity defect region prevails whose maximum is near the upper boundary layer edge (Figure 7 *a, c* at  $x = 377$  mm). Downstream, for the localized disturbance that has interacted with the high-frequency wave, this region propagates far across the upper edge of the boundary layer showing that the 'head' of the structure comes out of the boundary layer (Figure 7 *d*, at  $x = 480$  mm). The disturbance remains damped inside the boundary layer (Figure 7 *b*). The emergence of the 'head' of the increasing  $\Lambda$ -structure beyond the upper edge of the boundary layer was mentioned in ref. 14 (Figure 8).

Consider in detail the figure of isolines of velocity fluctuations in the plane  $y-t$  at  $x = 377$ ,  $480$  mm and spanwise co-ordinate  $z = 0$  mm. The structure of the damped localized disturbance at  $x = 377$  and  $480$  mm (see Figure 7 *a, b*) does not change. Considerable changes take place when the localized disturbance is superimposed by a high frequency wave. The 'head' of the structure comes close to the upper edge of the boundary layer, and several closed regions of isolines appear with defect and velocity excess (see Figure 7 *d*, at  $x = 480$  mm).

Thus, we may state that the structure of the damped localized disturbance and its interaction with a high frequency wave are two counter-rotating vortices ('legs') ending with the 'head'. The difference is that in the first case a disturbance does not pass the boundary layer edge and damps downstream, whereas in the second case a disturbance 'head' passes the boundary layer and the disturbance is transformed to a turbulent spot downstream.

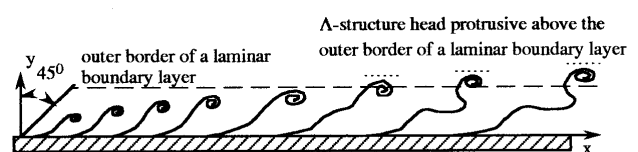


**Figure 8.** Sketch of the increasing  $\Lambda$ -structure development downstream in a laminar boundary layer (sketch is taken from the work ref. 14).

To understand better the structure of these two disturbances, measurements of the distribution of intensity and velocity fluctuations along the spanwise coordinate  $z$  for various positions normal to the surface  $x = 480$  mm were performed. The intensity distributions  $A = f(z, y)$  (see Figure 25 from ref. 18), and contour isolines of the velocity fluctuations of the damped localized disturbance in the transverse coordinate (Figure 9 *a, b*), confirm the characteristics of the given disturbance mentioned above. The structure of the damped disturbance presents probably two counter-rotating vortices ending with the 'head'. The 'head' of the structure is inside the boundary layer and the 'legs' have a weak bend towards the 'head', therefore typologically the disturbance reminds one of a 'hairpin' vortex rather than a  $\Lambda$ -vortex. The maximum width of the structure is approximately 25 mm (see figure 25 from ref. 18).

At the same distance from the leading edge ( $x = 480$  mm) the intensity distributions  $A = f(z, y)$  (see Figure 30 from ref. 18) and the contour isolines of the velocity fluctuations of the localized disturbance which has interacted with a high-frequency wave (see Figure 9 *c, d*) show that, at the periphery along the spanwise

coordinate two peaks with velocity defect are formed (see figure 30 from ref. 18). This means that the structure becomes wider on its 'legs' (approximately up to 35 mm), which have a horseshoe shape, and their intensity increases. One can observe the formation of the oblique waves at the edges of the  $\Lambda$ -structure. Beyond the boundary layer (see Figure 9 *d*, at  $y = 8.5$  mm) the structure becomes narrower (about 5 mm) with maximum amplitude in the plane of symmetry. One can conclude that typologically this disturbance reminds one rather of a classic  $\Lambda$ -structure (see visualization picture from ref. 12) than in the first case, though the source of generation of both disturbances is the same. The difference is that in the latter case the localized damped disturbance is superimposed by a secondary high-frequency wave. Their interaction led to the fact that the development of the secondary disturbance on the 'legs' of the structure, which is similar to the development of secondary disturbances in stationary vortices<sup>19</sup> or streaky structures ('puffs')<sup>13,20</sup>, created conditions for a transfer of energy from the mean flow to the counter-rotating vortices ('legs'). As a result of this process, the disturbance intensity grows and the 'head' passes across the edge of the boundary layer.

It should be noted that the flow visualization picture of the transformation of an isolated structure into a turbulent spot, given in ref. 12, reflects the process of interaction of disturbances. Secondary disturbances developed on the 'legs' of the  $\Lambda$ -structure can be observed in the visualization of its development in a water channel (see Figure 40 in ref. 18). An illustrative topological scheme of a damped and increased  $\Lambda$ -structure, formed on the basis of present research and analysis, is shown in Figure 10.

#### Characteristics of development of periodic $\Lambda$ -structures and their interaction with a high frequency wave

As was shown above, an isolated  $\Lambda$ -structure may damp or increase in the process of its interaction with a high frequency disturbance. The development of the latter downstream leads to a formation of a turbulent spot. There is a question whether periodic  $\Lambda$ -structures, i.e. structures modelling  $K$ - or  $N$ -modes of transition, can damp and, in interaction with a high frequency secondary disturbance, turbulize the flow. To answer this question an experiment on the same model (see Figure 1) and under the same conditions was performed. Periodic  $\Lambda$ -structures with frequency  $f = 60$  Hz and high frequency disturbances with frequency 240 Hz were generated. Figure 11 shows oscilloscope traces of the development of damped periodic  $\Lambda$ -structures downstream and their interaction with a high frequency disturbance. It is seen that, when a high frequency

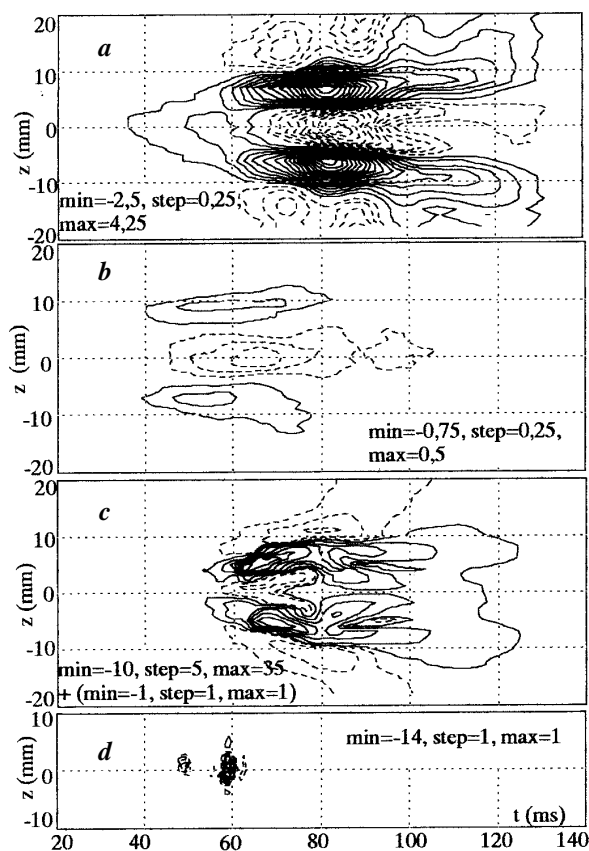


**Figure 9.** Contour diagrams of constant velocity fluctuations of the decreasing  $\Lambda$ -structure at  $y = 1.25$  mm (*a*), 5.0 mm (*b*) and its interaction with the high-frequency wave ( $f = 200$  Hz) at  $y = 1.25$  mm (*c*), 8.5 mm (*d*) in  $z$ - $t$  plane;  $U_\infty = 5.6$  m/s,  $x = 480$  mm.

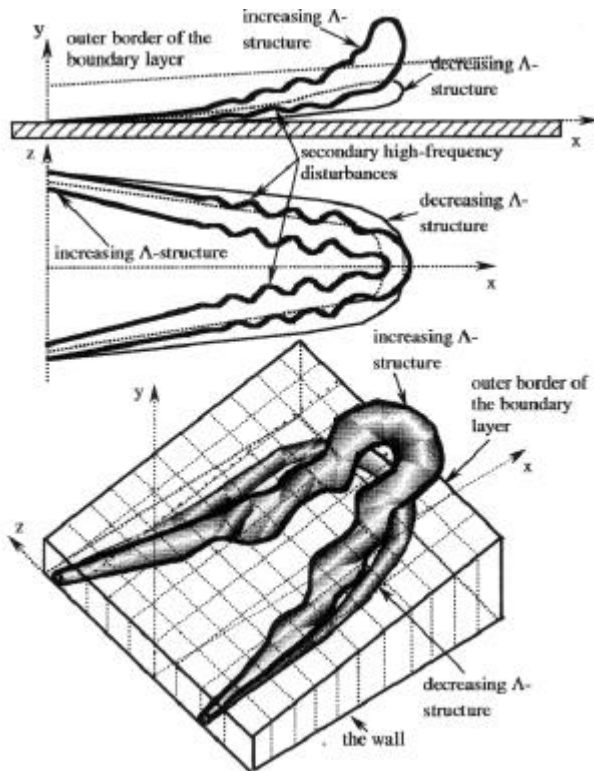


Figure 10. Sketch of the localized disturbance ( $\Lambda$ -structure-like).

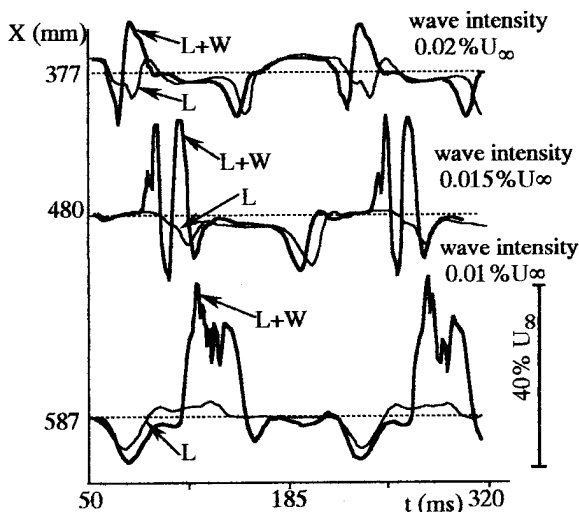


Figure 11. Oscilloscope traces of the periodic ( $f = 60$  Hz) decreasing  $\Lambda$ -structures (L) and their interaction with the high-frequency ( $f = 240$  Hz) wave (LW),  $U_\infty = 5.6$  m/s,  $y = y(u'_{\max})$ .

disturbance with amplitude lower than 1% is introduced in the boundary layer, it begins to interact with the  $\Lambda$ -structures, which then increase and are transformed into turbulent formations isolated in time. The same process is observed under 'natural' conditions when high frequency oscillations are not introduced<sup>21</sup>. Thus, as in a

previous case, periodic  $\Lambda$ -structures can damp and under certain conditions (such as when a high frequency disturbance is introduced) begin to increase and lead to flow turbulization. The data show that this is connected with the development of secondary high frequency disturbances on the 'legs' of the damped  $\Lambda$ -structure. The reason for an increase in the secondary disturbance may be a local transverse gradient of velocity  $\partial u/\partial z$  on the 'legs' of the structure. In the same way secondary high frequency disturbances are developed in flows modulated in a transverse direction by streaky structures ('puffs')<sup>20</sup> and stationary vortices<sup>19</sup>.

In conclusion we should mention the following. To control the process of a laminar-turbulent transition it is necessary to know its mechanism. In this respect research carried out in refs 13, 19, 20, 22–24, which showed the role of the transverse velocity gradient  $\partial u/\partial z$  in the development of secondary high-frequency disturbances in various three-dimensional flows, made a significant contribution to the study of the methods of control connected with the effect on the  $\partial u/\partial z$  gradient. In three-dimensional flows modulated in a transverse direction by streamwise stationary vortices of the Goertler type and 'cross-flow' vortices, secondary high frequency traveling disturbances can appear, develop and lead to transition depending on the value of the  $\partial u/\partial z$  gradient. Decrease in intensity of stationary vortices with riblets<sup>25</sup> or by local suction<sup>26</sup> can lead to a decrease of the  $\partial u/\partial z$  gradient, the development of secondary disturbances is then stopped or delayed, and transition is prevented. On the other hand, traveling localized disturbances of  $\Lambda$ -vortices, 'puffs' (streaky structures), etc. are streamwise vortices or streaks of accelerated or slow fluid, which as well as stationary vortices create spanwise modulation of a flow which is local in time and space. The gradient  $\partial u/\partial z$  may also be a reason for the development of the secondary disturbances in it. Investigation of the control of the transformation of  $\Lambda$ -vortices into turbulent spots by riblets<sup>27</sup> showed that the intensity of  $\Lambda$ -structure 'legs' decreased, and as a result the  $\partial u/\partial z$  gradient decreased too, and the development of the secondary disturbances was slower or stopped. Generation of the secondary vortices over the 'head' and on the 'legs' ceased, which led to delay in  $\Lambda$ -vortex transformation into a turbulent spot. The same result was obtained in research on the influence of riblets, spanwise wall oscillations and local suction on the development of secondary disturbances in 'puffs' (streaky structures)<sup>28,29</sup>.

Thus, research on the control of development and transformation of various streamwise vortices in turbulence has made it possible to confirm again one of the possible mechanisms of turbulization of a laminar flow through the process of development of the secondary high-frequency disturbances on the local gradients of velocity  $\partial u/\partial z$  formed in the modulation of the flow in a transverse direction by these structures.



## Conclusion

On the basis of research of  $\Lambda$ -structure transformation into a turbulent spot we can draw the following conclusions.

1. Localized disturbances of  $\Lambda$ -vortex type may damp as well as increase. Topologically both are counter rotating vortices ('legs') closed by the 'head' in the leading front. The difference is that the first one is close to a 'hairpin' vortex and disturbance does not pass across the upper edge of the boundary layer, whereas the second one has the form of the Greek letter  $\Lambda$  and the disturbance 'head' rises well out of the upper edge of the boundary layer.
2. The transformation of a  $\Lambda$ -structure into a turbulent spot is a result of the development of secondary high frequency disturbances on the 'legs', i.e. in the region of the maximum local velocity gradient  $\partial u/\partial z$ . This process may take place either in the development of a natural high frequency disturbance whose 'seed' may be in similar localized disturbances, or through the mechanism of disturbance interaction. The main condition for the realization of this mechanism is the value of the gradient  $\partial u/\partial z$  which is connected with the level of intensity of a localized disturbance and the periodicity of the counter-rotating vortices ('legs') in the spanwise coordinate.
3. The frequency of the secondary high frequency disturbance on the 'legs' of a structure decreases because of the constant stretching of a localized disturbance in a shear layer.
4. When a secondary disturbance develops it promotes energy transfer of a mean flow to low frequency disturbances ('legs' of the  $\Lambda$ -structure). The intensity of the 'legs' increases, which makes the 'h'  $\Lambda$ -structure come out across the upper edge of the boundary layer.
5. The mechanism of breakdown of periodic  $\Lambda$ -structures typical of  $K$ - and  $N$ -modes of transition, as in the case of destruction of an isolated  $\Lambda$ -structure or streaky structures, is connected with the development of the secondary high frequency disturbances in them.

1. Kozlov, V. V., Levchenko, V. Ya. and Sarik, V. S., *Izv. AS USSR, Mekhanika Zhidkosti i Gaza*, 1984, pp. 42–50 (in Russian).
2. Klebanoff, P. S., Tidstrom, K. D. and Sargent, L. M., *J. Fluid Mech.*, 1962, **12** 1–34.
3. Kachanov, Yu. S., Kozlov, V. V., Levchenko, V. Ya. and Ramazanov, M. P., *Izv. SB AS USSR, Ser. Tech. Sci.*, 1989, pp. 124–158 (in Russian).
4. Kachanov, Y. S., Kozlov, V. V. and Levchenko, V. Ya., *Izv. AS USSR, Mekhanika Zhidkosti i Gaza*, 1977, pp. 49–58 (in Russian).

5. Kachanov, Y. S. and Levchenko, V. Y., *J. Fluid Mech.*, 1984, pp. 209–247.
6. Elofsson, P. A., Doctoral Thesis, Royal Institute of Technology, Dept. of Mechanics, Stockholm, 1998.
7. Knapp, C. F. and Roache, P. J., *AIAA J.*, 1968, **6**, pp. 29–36.
8. Nishioka, M., Asai, M. and Iida, S., *Laminar-Turbulent Transition* (eds Eppler and Fasel), Springer-Verlag, Berlin, 1980, pp. 37–46.
9. Kachanov, Y. S., *J. Fluid Mech.*, 1987, pp. 43–74.
10. Rist, U. and Fasel, H., *Boundary Layer Transition and Control Conf.*, Royal Aero. Soc., Cambridge, 1991, pp. 25.1–25.9.
11. Wygnanski, I., Haritonidis, J. H. and Zilberman, H., *J. Fluid Mech.*, 1982, pp. 69–90.
12. Grek, G. R., Kozlov, V. V. and Ramazanov, M. P., *Modeling in Mechanics*, ITAM & CC SB RAS, Novosibirsk, 1989, vol. 3, pp. 46–60 (in Russian).
13. Chernorai, V. G., Bakchinov, A. A., Grek, G. R. et al., Abstr., 4th Siberian Seminar Stability of Homogeneous and Heterogeneous Fluids, Novosibirsk, 1997, pp. 100–101 (in Russian).
14. Acarlar, M. S. and Smith, C. R., *J. Fluid Mech.*, 1987, **175**, 43–83.
15. Johansson, A. V. and Alfredson, P. H., *J. Fluid Mech.*, 1982, **122**, 295–314.
16. Bakchinov, A. A., Grek, G. R., Katasonov, M. M. and Kozlov, V. V., Preprint, ITAM SB RAS, Novosibirsk, 1997, p. 55 (in Russian).
17. Grek, H. R., Dey, J., Kozlov, V. V., Ramazanov, M. P. and Turchto, O. N., Rep. 91-FM-2, Indian Inst. of Science, Bangalore, 1991, p. 37.
18. Grek, G. R., Katasonov, M. M., Kozlov, V. V. and Chernorai, V. G., Preprint, ITAM, SB RAS, Novosibirsk, 1998, p. 40 (in Russian).
19. Bakchinov, A. A., Grek, H. R., Klingmann, B. G. B. and Kozlov, V. V., *Phys. Fluids*, 1995, pp. 820–832.
20. Bakchinov, A. A., Grek, G. R., Katasonov, M. M. and Kozlov, V. V., Proceedings of the Third International Conference on Experimental Fluid Mechanics, Korolev, Moscow region, 1997, pp. 28–33.
21. Matsui, T. and Okude, M., *Laminar-Turbulent Transition* (ed. Kozlov, V. V.), Springer-Verlag, Berlin, 1985, pp. 625–633.
22. Boiko, A. V., Kozlov, V. V., Syzrantsev, V. V. and Scherbakov, V. V., IUTAM Symposium Sendai/Japan (ed. Kobayashi, R.), Springer-Verlag, Berlin, 1995, pp. 289–295.
23. Kohama, Y., *Acta Mech.*, 1987, p. 21.
24. Kohama, Y., Saric, W. S. and Hoos, J. A., Proceedings of Boundary Layer Transition and Control, Royal Aeron. Soc., London, 1991, pp. 4.1–4.13.
25. Grek, G. R., Kozlov, V. V., Klingmann, B. G. B. and Titarenko, S. V., *Phys. Fluids*, 1995, **7**, 2504–2506.
26. Boiko, A. V., Kozlov, V. V., Syzrantsev, V. V. and Scherbakov, V. A., Abstr. of Reports of 4th Siberian Seminar, Novosibirsk, 1997, pp. 20–21 (in Russian).
27. Grek, G. R., Kozlov, V. V. and Titarenko, S. V., *J. Fluid Mech.*, 1996, **315**, 31–49.
28. Katasonov, M. M. and Kozlov, V. V., Abstr. of Reports 4th Siberian Seminar, Novosibirsk, 1997, p. 57 (in Russian).
29. Bakchinov, A. A., Katasonov, M. M., Alfredsson, P. H. and Kozlov, V. V., Papers of 5th International Seminar, Novosibirsk, 1998, pp. 63–68.

ACKNOWLEDGEMENT. This research was supported by the Russian Foundation for Basic Research (Grants No. 96-01-01892, 96-15-96310, 99-01-00591).